

Solar Based High Frequency AC link Inverter

Basavaraj malkapur¹, Nagabhushan patil²

¹P G scholar, ²Professor, ^{1,2}EEE department, P.D.A College of engineering, Gulbarga, Karnataka, India

Abstract - A solar based high frequency AC link inverter is proposed in this paper. The proposed inverter overcomes most of the problems associated with existing inverter topologies. The proposed inverter act as a partial resonant converter, while resonance it facilitates the zero-voltage turn-on of the switches. Hence switching losses are very less and negligible. The LC link has low reactive ratings and low power dissipation, frequency of the link can be very high as a result inductor size and weight become less. This paper presents the results of the simulation and experimental test along with a detailed design procedure of the prototype inverter.

Key words- solar base inverter, ac link, zero voltage switching, high frequency, simulink

1. INTRODUCTION

Solar power sources play important role in many of power systems. They can be used in distributed energy systems and microgrid power systems. Solar power is extracted by PV systems which provide the DC voltage as output but later we can convert this energy into suitable form with PV inverters. The inverters convert the DC voltage into AC form. Power electronics is an integral part of these distributed energy (DE) systems and adds costs as well as certain reliability issues [1]. The inverters are responsible for most of the photo voltaic (PV) systems, they are costly and complex and their current mean time to first failure is unacceptable. Sometimes inverter failures contribute to unreliable PV systems by this producer will lose his confidence in renewable technology.

To achieve long-term success in the PV industry, new power converters with higher reliability and longer lifetimes are required [1]. In past days, inverters are designed with centralized converter-based PV system. In this, PV modules are connected to a three phase voltage-source inverter coupled with low frequency transformers. But these transformers are having large size and low efficiency. Later these are replaced by multiple-stage conversion system which includes a dc-ac voltage source inverter and a dc-dc

converter [6], [9]. But this topology offered some drawbacks such as bulky electrolytic capacitors which reduce the life of inverter. Also it reduced the efficiency of overall system [2], [3].

To overcome all these problems and to achieve reliability in the inverter system, a solar based high-frequency AC-link is proposed. This inverter which overcomes most of the problems compare to existing inverters. Also it reduces the cost and size of the inverter. The proposed inverter operating at zero voltage and zero currents switching hence the losses are neglected [1], [2]. It is partially resonant converter [2], [7].

2. PROPOSED INVERTER TOPOLOGY

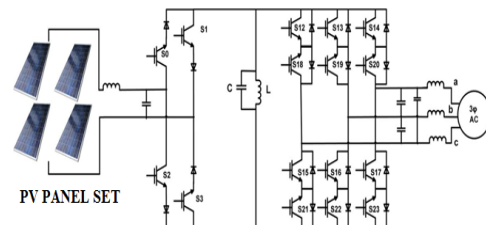


Fig 1: proposed circuit diagram [1]

Fig. 1 represents the proposed PV inverter diagram. It consist of four unidirectional switches forming the PV switch bridge interface the PV modules and six bidirectional switches forming the ac-side switch bridge connect the link to the load. The unidirectional switches at the PV side would replaced by bidirectional switches during grid fault. In such case, the inverter is required to inject reactive power [1]. The converter transfers power entirely through the link inductor. In this inverter, the switch is the dc-ac buck-boost converter in which the link is charged through the PV and then discharged into the load. The Charging and discharging takes place through link and link frequency generally more than line frequency. The Complimentary switches on each leg facilitate the charging and discharging of the link in a reverse direction. The alternating current of the link results in better utilization of the inductor and capacitor.

Fig.2. depicts the link current in a soft-switching ac-link buck-boost inverter [1], [3]. Here, between each

charging and discharging mode, there is a resonating mode during which none of the switches can conduct and the LC link resonates to provide zero-voltage turn-on of the switches. The input and output current pulses are forming due to alternating charge and discharge functions have to be precisely modulated to get desired levels. In order to control the output current and minimize harmonics, the discharging mode has to split into two modes as shown in fig 3.

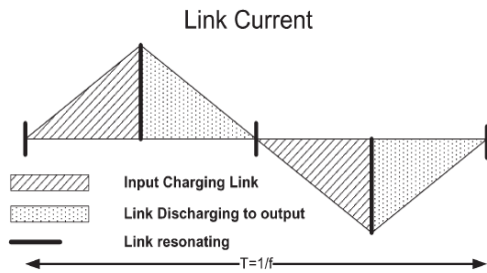


Fig. 2 link current in ac-link buck-boost inverter.

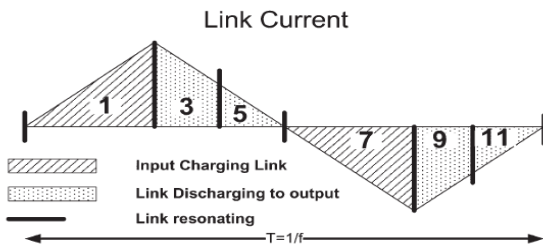


Fig.3. Link current in the proposed inverter. [1]

The general control strategy is to turn on each switch such that its turn-on occurs at zero voltage and to turn off the switches when the input or output currents meet their required level and soft-switched optimized structures leads to higher link frequencies. So filter capacitors are placed across the input and output terminals. The basic operating modes and relevant waveforms of this inverter are explained, the link cycle is divided into 12 modes, with six power transfer modes and six resonating modes [1], [3].

2.1 Mode 1 (Energizing):

Before the start of mode 1, switches S0 and S3 on the PV switch bridge are activated. However they do not immediately conduct since they are reverse biased. Once the link voltage becomes equal to the PV voltage, the proper switches S0 and S3 are forward biased with initiating mode 1. The conducting switches are shown in fig. 4.

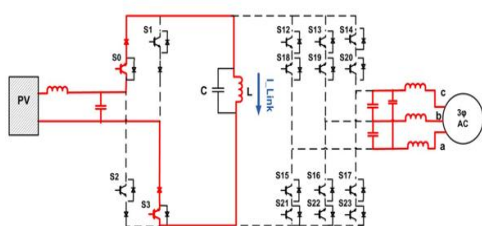


Fig.4, mode 1 operation (energizing)

This results in the zero-voltage turn-on of S0 and S3. The simple equivalent circuit is shown in Fig. 11 (a), can be used to analyze the circuit during mode 1. The link current (i_{Link}) during mode 1 can be calculated using the following:

$$V_{PV} = L \frac{di_{Link}(t)}{dt} \tag{1}$$

$$i_{Link}(t) = \frac{1}{L} \int_0^t V_{PV} dt = \frac{V_{PV} \times t}{L} + i_{Link}(0). \tag{2}$$

In equation (1) and (2), L and V_{PV} are the link inductance and PV voltage respectively. During this mode operation, the link voltage is equal to V_{PV} . The link is charged over a cycle to meet its reference value. The switches located on the PV switch bridge are then turned off. As mentioned earlier, the link capacitor acts as a buffer across the switches during their turn-off, which results in low turn-off losses.

2.2 Mode 2 (Partial resonance):

During mode 2 operation, none of the switches conduct and the link resonates and link voltage decreases. In this mode, the circuit behaves as a simple LC circuit as depicted in Fig. 11(b). The following equation describes the behavior of the LC circuit ($i_c(t)$), $V_{Link}(t)$ and C are the capacitor current, link voltage and link capacitance respectively. The capacitor current is given by,

$$i_c(t) = C \frac{dV_{Link}(t)}{dt}. \tag{3}$$

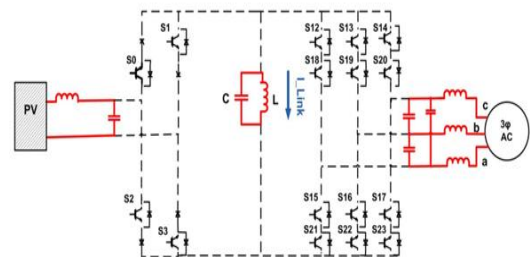


Fig.5, mode 2 operation (partial resonance)

As shown in fig.11 (b), the current passing through the capacitor is equal to $-i_{Link}(t)$ and the inductor current is positive which resulting in negative $dV_{Link}(t)/dt$. This implies that the link voltage is decreasing. Once the link voltage becomes negative, the controller determines which output phase pairs have to be charged through the link during modes 3 and 5. During mode 2, the output switches S18, S22, and S23 which are supposed to conduct. Once the link voltage reaches $V_{ab}-0$ switches S18 and S22 will be

forward biased and will start to conduct with initiating mode 3. This theme is given as shown in above fig.5.

2.3 Mode 3 (De-energizing): during mode 3 operation, the output switches S18 and S22 are turned on at zero voltage to allow the link to be discharged into the chosen phase pair until the current of phase b meets its reference value. At this point, switch S22 will be turned off and initiating another resonating mode. This mode operation is given in fig. 6.

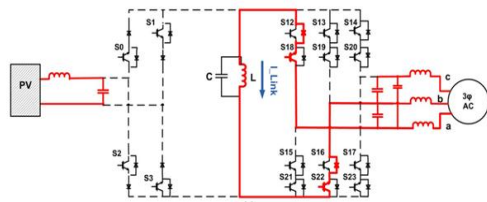


Fig.6, mode 3 operation (de-energizing)

2.4 Mode 4 (Partial resonance): during mode 4 operation, the link is allowed to swing to the voltage of the other output phase pair of the mode 2. Fig.11 shows the link voltage swings from $V_{ab}-o$ to $V_{ac}-o$. in this mode operation switches S18,S22,S23 supposed to conduct. The mode switches operation given in fig.7.

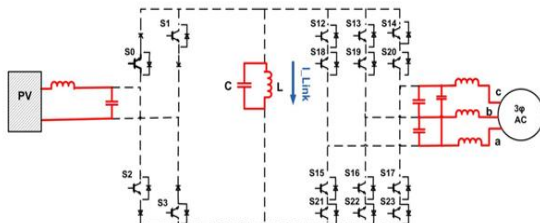


Fig.7, mode 4 (partial resonance)

2.5 Mode 5(De-energizing): During mode 5 operation, the AC link discharges to the selected output phase pair until there is just sufficient energy left in the link to swing to a predetermined voltage (V_{max}), which is slightly higher than the maximum input and output line-to-line voltages. At the end of mode 5 operation, all the switches are get turned off and allow the link to start next mode operation. The switches operation of mode 5 is shown in fig.8.

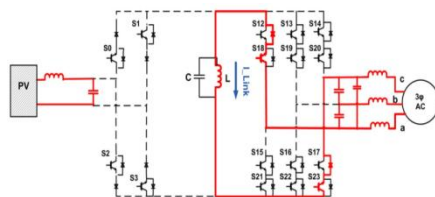


Fig.8. mode 5 operation (de-energizing)

2.6 Mode 6 (Partial resonance): In this mode of operation switches S18,S22,S23 supposed to conduct.The link voltage swings to maximum voltage value V_{max} and its absolute value decreases. This mode of operation is given in fig.3.9. Proper switches which are supposed to conduct during mode 7 are turned on during this mode but they do not conduct as they are reversed biased. Modes 7 to 12 are similar to modes 1 to 6, except that the link charges and discharges in the reverse direction.

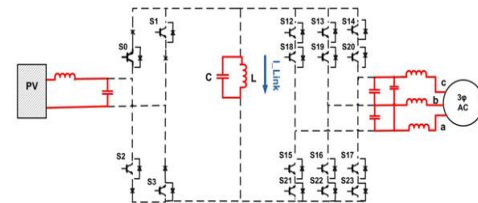


Fig.9, mode 6 (partial resonance)

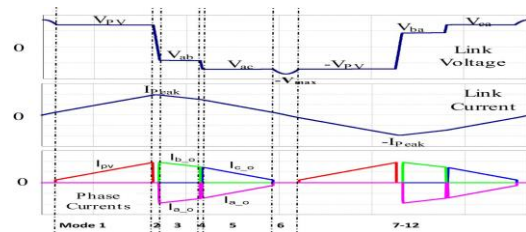


Fig.10, voltage and current waveforms of different modes of operation. [1], [3]

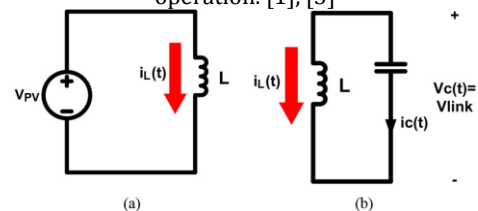


Fig.11, equivalent circuit during (a) energizing and (b) resonating modes [1]

3. SOFTWARE IMPLEMENTAION

Simulink includes a comprehensive block library of toolboxes for both linear and nonlinear analyses. Models are hierarchical, which allow using both top-down and bottom-up approaches. As Simulink is an integral part of MATLAB, it is easy to switch back and forth during the analysis process and thus, the user may take full advantage of features offered in both environments. The main advantage of SIMULINK over other programming software's is that, instead of complication of program code, the simulation is build up systematically by means of basic functional blocks.

3.1 Simulation for proposed system

Fig.12 shows the simulation diagram for the proposed system using MATLAB Simulink R2010a version by using different Sim power system components.

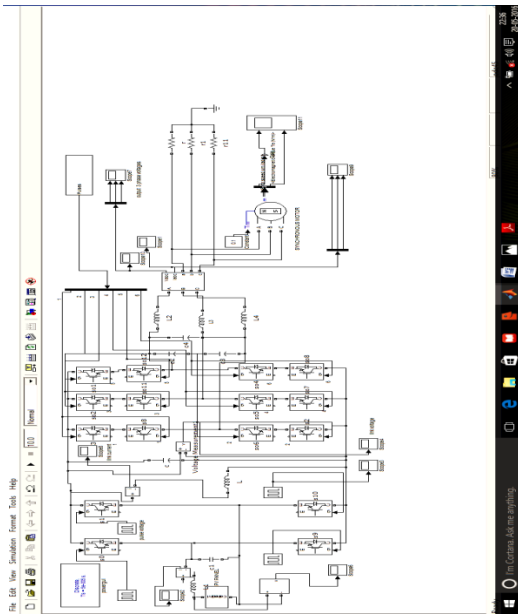


Fig.12 Simulation model of proposed inverter

Fig.13 efficiency v/s output power graph

Simulation model tested and fabricated in MATLAB R2010a, the snap charts of input, output, link voltages are given are shown in following figures for different input voltages

1) Simulation results for input DC 50v:



Fig 14, waveform of input 50V DC

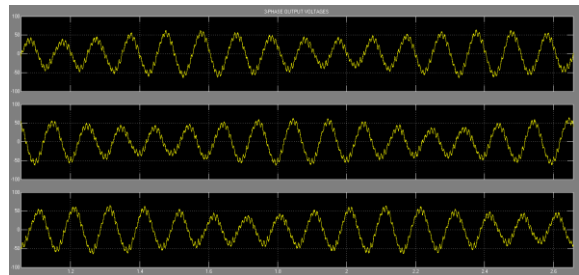


Fig.15 output voltage waveforms for 50V DC input

3.2 Simulation results

Table 1 shows the different efficiency values for different input and output voltage, the overall efficiency is around 90% to 93.33%.

TABLE 1 Efficiency table for different voltages

Sl no.	Input voltage (volts)	Output voltage (volts)	Input power (watts)	Outpour power(watts)	Efficiency (η)
1	50	40	15	13.5	90
2	100	80	30	28	93.33
3	150	140	105	98	93.33

And one more significant phenomenon we observed here is that, the AC link frequency is very high and constant irrespective of voltage changes. The AC link parameters are inductor and capacitor and correspond set values are 11mH and 0.8μF respectively. The link frequency obtained here is 2 MHz which is very much higher compared to line frequency. The graph for efficiency verses output power is drawn. Efficiency curve goes on increasing for low power, at certain rate it becomes maximum.

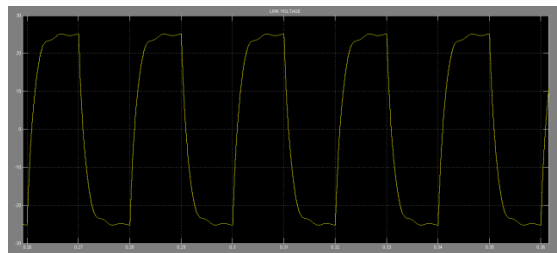
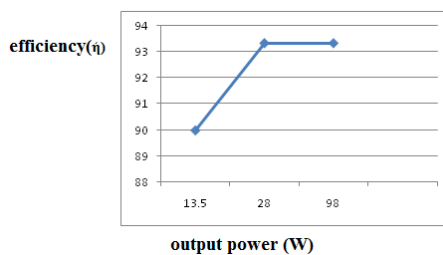


Fig. 16 AC link voltages for input 50V DC

2) simulation results for 100V DC input:

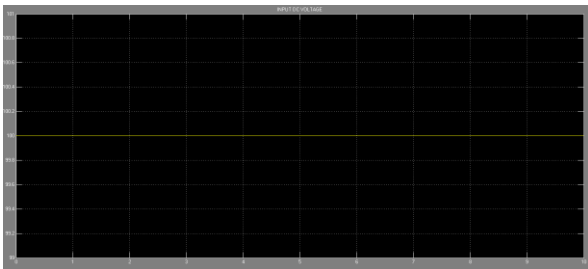


Fig.17 waveform for 100V DC input voltage

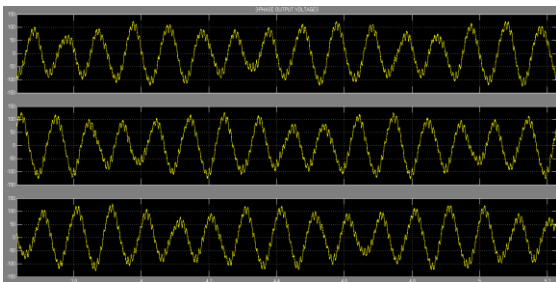


Fig.18 Output voltages for 100V DC input Voltage

3) Simulation results for 150 DC input :

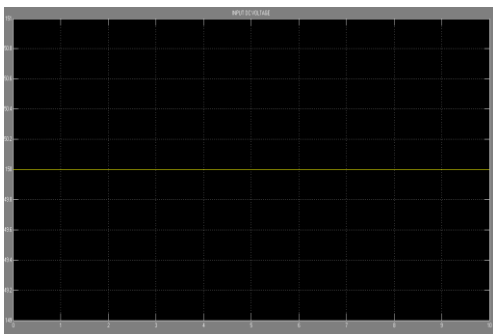


Fig.19. waveform for 150 DC input voltage

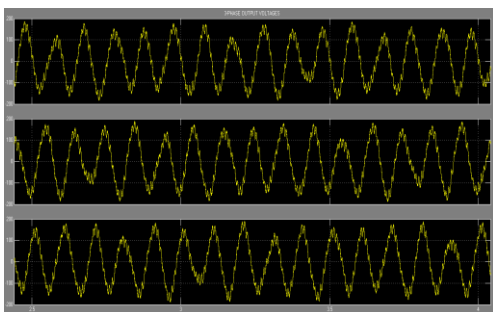


Fig.20 Output voltages for DC 150V input

4. HARDWARE IMPLEMENTATION

The Solar based high frequency AC link inverter module for a photovoltaic system is done and the developed hardware is tested with constant load. The proposed hardware system is implemented by PIC-microcontroller 16F877A. The developed hardware system is tested in power electronics laboratory. The test is carried out on an inductive-resistive load. Input and output voltage is tabulated in table 2. The set parameter values for inductor and capacitor for AC link are 1.8mH and 33uF respectively. Also corresponding link frequency has calculated. Figure 21 shows the photograph of the proposed system.



Fig.21 hardware setup of the proposed system

Table 2 Efficiency table for input and output voltages.

Sl no	Input voltage (V)	Output voltage (V)	Input power (W)	Output power (W)	Efficiency (ij)	Link Frequency (KhZ)
01	12	11.5	34.8	32.5	93.4	6.25

From above table readings, it is come to know that, the efficiency of the hardware is around 93% and link frequency is 6.25 KHz which is much compared to line frequency. This frequency shows that, inductor size become compact. Hence the losses are less. And efficiency of inverter is more. After testing required hardware results are obtained, they are as shown in following figures

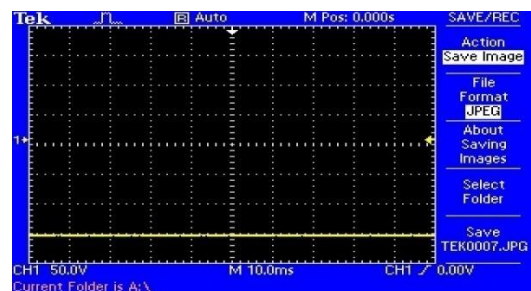


Fig.22 DC input voltage

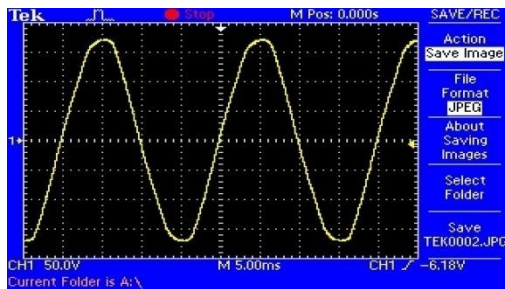


Fig.23 ouput voltage

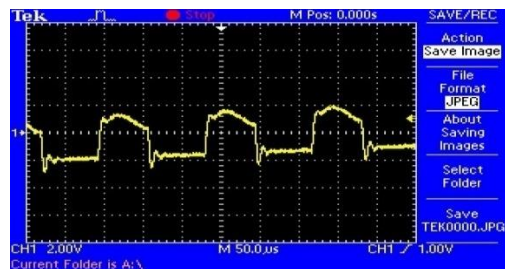


Fig.24 AC Link voltage

Advantages:

- Eliminates switching losses.
- Less Electromagnetic interference (EMI).
- The Variation of the link Frequency is less.
- Switching losses are less and neglected
- Efficiency is more compared other existing inverters.

Applications:

1. We can be used it in DC fans.
2. This can be used in LED lighting system.
3. Also can be used in 24V BLDC motor.

CONCLUSION

A new topology of solar based high frequency AC link inverter was successfully implemented in this work. The high-frequency AC-link is composed of a small inductor-capacitor pair in parallel. Both of the link components work at high frequency ac currents and voltages, so they are small in size and low in weight. And link frequency is very high compared to line frequency. By this, the considerable losses are highly reduced and desired efficiency is achieved. The Simulation is carried out for the inputs 50V, 100V and 200V, resulting output voltages 40V, 80V and 150v respectively. For the same, the hardware experiment is conducted for the input 12V and resulted output is 11.5V for AC link inverter. Ultimately efficiency of the inverter is around 94% from the results analysis. Hence proposed inverter topology is best suitable for 90% of low power applications.

REFERENCES

[1] Mahshid Amirabadi, Anand Balakrishnan, Hamid A. Toliyat and William C. Alexander, *Member, IEEE* "High-

Frequency AC-Link PV Inverter" *IEEE transactions on industrial electronics*, vol. 61, no. 1, january 201

[2] T. Kerekes, R. Teodorescu, P. Rodríguez, G. Vázquez, and E. Aldabas, "A new high-efficiency single-phase transformerless PV inverter topology," *IEEE Trans. Ind. Electron.*, vol. 58, no. 1, pp. 184–191, Jan. 2011.

[3] M. Amirabadi, A. Balakrishnan, H. A. Toliyat, and W. Alexander, "Soft switched AC-link direct-connect photovoltaic inverter," in *Proc. IEEE Int. Conf. Sustain. Energy Technology*, 2008, pp.

[4] Aleksey Trubitsyn, Brandon J. Pierquet, Alexander K. Hayman, Garet E. Gamache, Charles R. Sullivan, David J. Perreault "High-Efficiency Inverter for Photovoltaic Applications", 2010 IEEE Energy Conversion Congress and Exposition, pp. 2803-2810, Sept. 2010

[5] Eftichios Koutroulisa, John Chatzakisa, Kostas Kalaitzakisa, Stefanos Maniasb, "System for inverter protection and real-time monitoring" *Microelectronics Journal* 34 (2003) 823

[6] S. Chakraborty, B. Kramer, and B. Kroposki, "A review of power electronics interfaces for distributed energy systems towards achieving low-cost modular design," *Renew. Sustain. Energy Rev.*, vol. 13, no. 9, pp. 2323–2335, Dec. 2009.

[7] H. A. Toliyat "Partial Resonant ac Link Converters" *Journal of Electrical Systems and Signals*, Vol. 1, No. 1, Mar. 2013

[8] M. Amirabadi, H. A. Toliyat, and W. C. Alexander, "Battery-utility interface using soft switched AC link buck-boost converter," in *Proc. IEMDC*, 2009, pp. 1299–1304.

[9] G. Grandi, C. Rossi, D. Ostojic, and D. Casadei, "A new multilevel conversion structure for grid-connected PV applications," *IEEE Trans. Ind. Electron.*, vol. 56, no. 11, pp. 4416–4426, Nov. 2009.

[10] Y. Huang, F. Z. Peng, J. Wang, and D. W. Yoo, "Survey of the power conditioning system for PV power generation," in *Proc. IEEE PESC*, Jun. 18–22, 2006, pp. 1–6.

[11] S. Atcitty, J. E. Granata, M. A. Quinta, and C. A. Tasca, "Utility-scale gridtied PV inverter reliability workshop summary report", Sandia National Labs., Albuquerque, NM, USA, SANDIA Rep. SAND2011-4778

[12] S. Jain and V. Agarwal, "An integrated hybrid power supply for distributed generation applications fed by nonconventional energy sources," *IEEE Tran. Energy Conversion*. vol. 23, no. 2, pp. 622–631, Jun. 2008.

Author's Profile:

Basavaraj malkapur, PG Scholar,
Dept of EEE, Poojya Doddappa
Appa College of Engineering,
Gulbarga, Karnataka, India,
E-mail: basavarajmalkapur@gmail.com



Nagabhushan patil, Professor,
Dept. of EEE, Poojya Doddappa
Appa College of Engineering,
Gulbarga, Karnataka, India,
E-mail: nappdaceg@yahoo.co.in